Available online at www.sciencedirect.com

SciVerse ScienceDirect

Advances in Space Research 51 (2013) 395–410

ADVANCES IN SPACE RESEARCH (a COSPAR publication)

www.elsevier.com/locate/asr

# Solar and interplanetary precursors of geomagnetic storms in solar cycle 23

J. Uwamahoro [a,b,*], L.-A. McKinnell [b,c]

[a] Kigali Institute of Education [KIE], Department of Physics, P.O. Box 5039, Kigali, Rwanda
[b] South African National Space Agency [SANSA], Space Science, P.O. Box 32, Hermanus 7200, South Africa
[c] Department of Physics and Electronics, Rhodes University, P.O. Box 94, Grahamstown 6140, South Africa

Received 26 November 2011; received in revised form 23 September 2012; accepted 24 September 2012
Available online 3 October 2012

**Abstract**

Estimating the magnetic storm effectiveness of solar and associated interplanetary phenomena is of practical importance for space weather modelling and prediction. This article presents results of a qualitative and quantitative analysis of the probable causes of geomagnetic storms during the 11-year period of solar cycle 23: 1996–2006. Potential solar causes of 229 magnetic storms ($Dst \leqslant -50$ nT) were investigated with a particular focus on halo coronal mass ejections (CMEs). A 5-day time window prior to the storm onset was considered to track backward the Sun's eruptions of halo CMEs using the SOHO/LASCO CMEs catalogue list. Solar and interplanetary (IP) properties associated with halo CMEs were investigated and correlated to the resulting geomagnetic storms (GMS). In addition, a comparative analysis between full and partial halo CME-driven storms is established. The results obtained show that about 83% of intense storms ($Dst \leqslant -100$ nT) were associated with halo CMEs. For moderate storms ($-100$ nT $< Dst \leqslant -50$ nT), only 54% had halo CME background, while the remaining 46% were assumed to be associated with corotating interaction regions (CIRs) or undetected frontside CMEs. It was observed in this study that intense storms were mostly associated with full halo CMEs, while partial halo CMEs were generally followed by moderate storms. This analysis indicates that up to 86% of intense storms were associated with interplanetary coronal mass ejections (ICMEs) at 1 AU, as compared to moderate storms with only 44% of ICME association. Many other quantitative results are presented in this paper, providing an estimate of solar and IP precursor properties of GMS within an average 11-year solar activity cycle. The results of this study constitute a key step towards improving space weather modelling and prediction.


*Keywords:* Geomagnetic storms; Coronal mass ejections; Solar cycle 23; Space weather

## 1. Introduction

CMEs are transient expulsions of plasma and magnetic fields from the Sun which are responsible for strong IP disturbances and their subsequent non-recurrent and recurrent geomagnetic storms (Sheeley et al., 1985; Crooker and McAllister, 1997). GMS are strong perturbations of the Earth's magnetosphere that can affect in various ways our modern technological society. Details pertaining to various space weather impacts on modern technology can be found for example in Lanzerotti (2007). Therefore, the ability to estimate the storm efficiency of solar and IP events is of practical importance in the domain of space weather prediction.

The main sources of GMS are: (a) CME eruptions from the Sun and (b) the CIRs that result from an interaction between the fast and slow solar wind (SW) originating from coronal holes. These two phenomena evolve into geoeffective SW conditions, producing moderate to intense GMS when there is an enhanced and long lasting IP magnetic field (IMF) in the southward direction (e.g., Gonzalez et al., 1994; Tsurutani and Gonzalez, 1997; Richardson et al., 2002; Richardson et al., 2006; Gopalswamy et al.,

* Corresponding author at: Kigali Institute of Education [KIE], Department of Physics, P.O. Box 5039, Kigali, Rwanda. Tel.: +250 0255100589; fax: +250 586890.
*E-mail address:* mahorojpacis@gmail.com (J. Uwamahoro).

0273-1177/$36.00 © 2012 COSPAR. Published by Elsevier Ltd. All rights reserved.
http://dx.doi.org/10.1016/j.asr.2012.09.034

2007; Zhang et al., 2007; Richardson and Zhang, 2008; Echer et al., 2008; Yermolaev and Yermolaev, 2010 and references therein). However, despite the fact that halo CMEs are known to be the major sources of GMS, there is no one to one association between a CME eruption and the storm occurrence. Hence the prediction of GMS based only on CME observations remains difficult and often lead to false alarms.

Currently, space-based instruments allow advanced observations and understanding of storm events occurring on the Sun. The Solar and Heliospheric Observatory/Large Angle and Spectrometric Coronagraph (SOHO/LASCO) has been detecting CME occurrence on the Sun since the rise of SC 23 (Brueckner et al., 1995). To date, the Solar-Terrestrial Relations Observatory (STEREO) twin spacecraft allow the CME tracking from the Sun to Earth, and the collected data will contribute towards improving the predictability of geoeffective CMEs (Messerotti et al., 2009). The CMEs that appear to surround the occulting disk of the observing coronagraphs are known as halo CMEs among which, those originating from the visible solar disc and that are earth-directed have the highest probability of impacting the Earth's magnetosphere (Webb et al., 2000). In their study, Webb et al. (2000) and Cyr et al. (2000) used 140° and 120° respectively as a threshold apparent angular width (AW) to define halo CMEs, while a study by Wang et al. (2002) considered a halo CME to be one with an apparent AW greater than 130°. Recently, Wang et al. (2011) defined halo CMEs as those having AW > 100°. In this study, halo CMEs were defined following a categorization by Gopalswamy et al. (2007): full halo CMEs (F-type) with AW of 360°, and partial halos (P-type), those with an apparent AW of $120^0 \leqslant W \leqslant 360°$.

Over an 11-year period of solar cycle (SC) 23 [from January 1996 to December 2006], 393 full halo CMEs were identified representing 3.4% of all 11683 CMEs recorded. During the same period, the number of partial halo CMEs was 840. Therefore during the same period, LASCO observed 1233 (10.5%) halo CMEs of which 393 (31.8%) were full halo CMEs and 840 (68.2%) partial halo CMEs. As illustrated in Fig. 1, the occurrence of full halo CMEs varies in steps with the occurrence of GMS for the period of 1996–2006. However, not all halo CMEs are geoeffective. By simply considering the total number of investigated GMS events (244) during the period of study, the storm effectiveness of halo CMEs can be roughly estimated at about 20%. It must be noticed that a number of storm events are often observed without any link to frontside halo CMEs (Schwenn et al., 2005). As mentioned by Gopalswamy et al. (2007), the non halo CMEs can also cause GMS if they arrive at the Earth with an enhanced southward component of the IP magnetic field at high speed. Indeed both intense and moderate GMS can also be caused by CIRs (Richardson et al., 2006; Zhang et al., 2007).

During the last decade, there has been increasing research with focus towards estimating the geoeffectiveness of solar phenomena. A statistical study by Wang et al. (2002) investigated the geoeffectiveness of frontside CMEs during the rise of SC 23. The geoeffectiveness of both full and partial halo CMEs has been discussed in detail in papers by Gopalswamy et al. (2007) and Gopalswamy (2009). A research article by Zhang et al. (2007) presented results of a study that was aimed to investigate the solar and interplanetary causes of major GMS events ($Dst \leqslant -100$ nT) during the period 1996–2005. Despite many efforts regarding this subject, there are persistent discrepancies in the various estimations of storm effectiveness of solar and IP events. The differences in the geoeffectiveness estimations may either be due to the methods used to analyse the data (Yermolaev et al., 2005), or otherwise due to different definitions given to halo CMEs (Gopalswamy, 2009). For this study, the term geoeffectiveness used refers to the efficiency of magnetic storms ($Dst \leqslant -50$ nT) occurrence as a the result observed solar and IP probable causes (Yermolaev and Yermolaev, 2010).

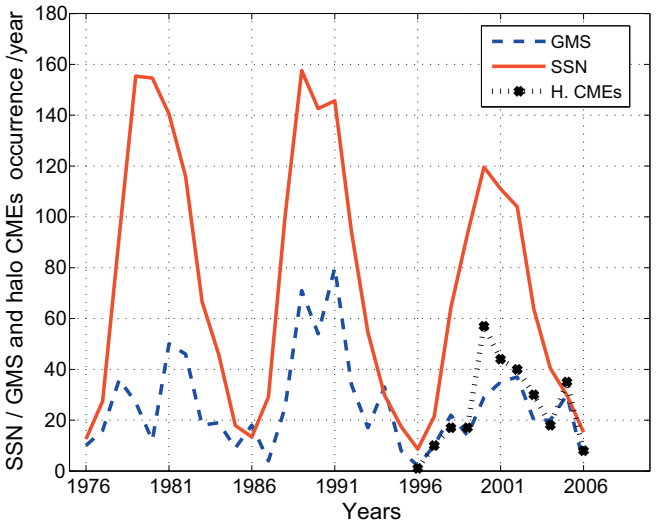


Fig. 1. The correlation between solar activity cycle (in terms of sunspot number) and the occurrence of GMS during the last three SCs (SC 21, SC 22 and SC 23). For SC 23, the frequency occurrence of GMS is shown for comparison with the occurrence of halo CMEs.

The focus is to investigate halo CMEs and associated solar and IP properties that were most likely causes of the 229 storm events identified during the period 1996–2006. Hence, unlike the analysis by Zhang et al. (2007) which involved only 88 major storms ($Dst < -100$ nT), this study includes an additional quantitative estimate of the solar and IP properties that were associated with moderate GMS during SC 23. In addition, this study compares the magnetic storm effectiveness of both full and partial halo CMEs, as well as their associated IP properties.

## 2. Data and methods

### 2.1. Selection of GMS events

Phenomena leading to GMS evolve normally in the Sun-Earth direction, however it is common to proceed from

Earth to the Sun when analysing geoeffectiveness of solar events (Zhang et al., 2007). Geomagnetic indices such as the disturbance storm time (*Dst*) and the *Kp* indices are commonly used to quantify the level of geomagnetic response to solar transient phenomena. For this study, the *Dst* index was used for the selection of storm events. The *Dst* index is a measure of the horizontal component of the Earth's magnetic field at low to mid-latitudes. It is a proxy for deviation of the horizontal component at the equator from a quiet day and is generally considered as a measure of the ring current. In the selection of GMS events, an effort has been made to select clearly isolated GMS periods without considering any single event with $Dst \leqslant -50$ nT as a separate storm. This is because a given isolated storm can be characterised by a multiple period with $Dst \leqslant -50$ nT especially during high magnetic activity periods.

Only moderate to intense GMS events ($Dst \leqslant -50$ nT) were considered leaving out the minor storms. The storm classification, e.g., Loewe and Prölss (1997, 2007) was followed to categorise moderate storms (with $-100\,\text{nT} \leqslant Dst \leqslant -50$ nT) and intense storms with $Dst \leqslant -100$ nT. A table showing the solar and IP sources of major GMS in SC 23 (1996–2005) was presented in a study by Zhang et al. (2007). Table 1 is an extension of the one by Zhang et al. (2007) and includes moderate storms. It contains 244 GMS events and probable associated halo CMEs from January 1996 to December 2006. Columns 2 and 3 of Table 1 indicate the storm time and the peak minimum value of the *Dst* index respectively. The *Dst* index data set used were obtained from the National Geophysical Data Center (NGDC), available on the website: http://www.ngdc.noaa.gov/stp/geomag/dst.html.

### 2.2. IP signatures of geoeffective solar events

Solar disturbances are transported from the Sun to near-Earth via the SW. The CME structures in IP medium (at about 1 astronomical units or 1 AU) are known as interplanetary counterpart of CMEs or ICMEs. ICMEs which often may contain strong and long lasting southward component of the IMF lead to intense GMS (Gosling et al., 1990). The geoeffectiveness of an ICME has been found to be correlated with the negative Z-component of the IMF ($B_s$) or $E_y \backsimeq VB_s$ (Richardson and Cane, 2011), where $E_y$ is the $y$ component of the SW convective electric field $E = -VB$). A catalogue of ICME events, their associated properties as well as their geomagnetic effect can be found in Richardson and Cane (2010), and its updated version is also available online: (see: http://www.srl.caltech.edu/ACE/ASC/DATA/level3/icmetable2.htm).

Table 1 is a subset of the Richardson and Cane (RC)'s table (catalogue) with two major differences:

- The RCs table is based on ICME events and not on GMS events. Therefore, Table 1 contains additional 92 storm events which are not listed in RCs table. In the last columns of Table 1 which indicates the start time of the observed ICME, storm events which are missing in the RCs table are indicated with *m*.
- Contrary to the RCs table, Table 1 concerns only moderate and intense storms. All events with $Dst > -50$ nT do not appear in Table 1 and were not involved in this analysis.

Fig. 2 illustrates the perturbations induced in the SW and the IMF following the near-Earth passage of an ICME.

A geoeffective SW is characterised by a prolonged and enhanced *Bs* that allows efficient SW energy transport into the Earth's magnetosphere. The intensity of a magnetic storm depends mainly on the magnitude of $B_s$ and the speed with which the CME impacts the Earth magnetosphere. To investigate the geoeffective SW conditions associated with GMS events, hourly averaged values of the SW speed and *Bs* were considered. The most recent peak values of *Bs* prior to the peak minimum *Dst* were used. For practical purpose, the SW velocity considered in this analysis corresponds to the time of peak minimum *Dst*. In Table 1, *Bs* and SW peak values are indicated in columns 4 and 5 respectively. The SW speed and *Bs* data used are in situ (measured values at 1 AU from various spacecrafts) data provided by the National Space Science Data Center (NSSDC) and were obtained via its OMNIWEB: http://www.nssdc.gsfc.nasa/omniweb.html.

### 2.3. Solar properties associated with geoeffective halo CMEs

A large AW of CMEs is often an indication that they are directed along the Sun-Earth line, with higher probability to impact the Earth's magnetosphere (Howard et al., 1982). The AW and first time of halo CME appearance in the LASCO coronagraphs are indicated in column 6 of Table 1. The AW of a CME is labelled FH (for full halo i.e., $W = 360°$) and PH for a partial halo ($120° \leqslant W \leqslant 360°$). In addition to their AW appearance in the coronagraphs, other geoeffective CME properties include their speed (see column 7 of Table 1) and their association with X-ray flares. As indicated by Kahler (1992), GMS and their associated IP disturbances can be traced back directly to large flares. Kahler (1992) also noted that the surface location of a long duration flare can be considered as the source region of the associated CME. Hence, the association of X-ray flares with halo CMEs can help to identify the solar surface location origin of CMEs (Gopalswamy, 2009). In this analysis, we followed the same criteria as in Gopalswamy et al. (2007) and considered a time range of ±0.5 h to decide the association of halo CME eruption with flare occurrence. The X-ray flare class, level of intensity as well as the solar surface coordinates are indicated in columns 8 and 9 of Table 1.

X-ray flare classification is based on the order of magnitude of the peak burst intensity (*I*) measured by the Geostationary Operational Environmental Satellite (GOES)

Table 1
GMS events with associated solar and IP properties in SC 23: 1996–2006.

| E. No. | Storm time | *Dst* min. (nT) | Bz (nT) | Vsw (km/s) | CME /Time | V_cmes | XRFs | XRF_Loc. | ICME /start |
|---|---|---|---|---|---|---|---|---|---|
| *Year 1996* | | | | | | | | | |
| 1 | 13/01/96 – 11:00 | −90 | −8.2 | 387 | dg | – | – | – | – |
| 2 | 21/03/96 – 22:00 | −66 | −3.9 | 636 | – | – | – | – | m |
| 3 | 25/03/96 – 01:00 | −60 | −7.2 | 544 | dg | – | – | – | – |
| 4 | 15/04/96 – 00:00 | −56 | −7.2 | 589 | – | – | – | – | m |
| 5 | 23/10/96 – 04:00 | −105 | −11 | 634 | – | – | – | – | m |
| *Year 1997* | | | | | | | | | |
| 6 | 10/01/97 – 09:00 | −78 | −12.7 | 445 | FH:06/01 [15:10] | – | – | – | 10/01 [04:00] |
| 7 | 10/02/97 – 11:00 | −68 | −7.6 | 456 | FH:07/02 [00:30] | 490 | – | – | 10/02 [02:00] |
| 8 | 27/02/97 – 23:00 | −86 | −13.3 | 522 | – | – | – | – | – |
| 9 | 11/04/97 – 04:00 | −82 | −8.5 | 437 | FH:07/04 [14:27] | 878 | C6.8 | S30E19 | 11/04 [06:00] |
| 10 | 17/04/97 – 05:00 | −77 | −9.3 | 499 | – | – | – | – | m |
| 11 | 21/04/97 – 23:00 | −107 | −9.6 | 409 | – | – | – | – | 21/04 [10:00] |
| 12 | 15/05/97 – 12:00 | −115 | −23.9 | 447 | FH:12/05 [05:30] | 464 | C1.3 | N21W08 | 15/05/ [09:00] |
| 13 | 27/05/97 – 04:00 | −73 | −10.4 | 328 | – | – | – | – | 26/05/ [16:00] |
| 14 | 09/06/97 – 04:00 | −84 | −9.4 | 374 | – | – | – | – | 08/06 [18:00] |
| 15 | 03/09/97 – 22:00 | −98 | −15.8 | 487 | FH:30/08 [01:30] | 371 | – | – | 03/09 [13:00] |
| 16 | 01/10/97 – 16:00 | −98 | −9.5 | 483 | FH:28/09 [01:08] | 359 | – | – | 01/10 [16:00] |
| 17 | 11/10/97 – 03:00 | −130 | −10.3 | 422 | PH:06/10 [15:28] | 293 | – | S27W05 | 10/10 [11:00] |
| 18 | 25/10/97 – 03:00 | −64 | −9.1 | 428 | FH:21/10 [18:03] | 523 | C3.3 | N16E07 | 27/10 [00:00] |
| 19 | 07/11/97 – 04:00 | −110 | −12.5 | 456 | FH:04/11 [06:10] | 785 | X2.1 | S14W33 | 07/11 [19:00] |
| 20 | 23/11/97 – 06:00 | −108 | −12.8 | 500 | FH:19/11 [12:27] | 150 | C1.6 | N24E05 | 22/11 [19:00] |
| 21 | 11/12/97 – 10:00 | −60 | −11.2 | 332 | PH:06/12 [22:06] | 397 | – | – | 10/12 [18:00] |
| 22 | 30/12/97 – 19:00 | −77 | −10.4 | 352 | PH:26/12 [02:31] | 197 | – | – | 30/12 [10:00] |
| *Year 1998* | | | | | | | | | |
| 23 | 07/01/98 – 04:00 | −77 | −9.9 | 405 | FH:02/01 [23:28] | – | – | – | 07/01 [01:00] |
| 24 | 28/01/98 – 12:00 | −55 | −7.4 | 374 | FH:25/01 [15:26] | 693 | C1.1 | N21E25 | 29/01 [20:00] |
| 25 | 18/02/98 – 00:00 | −100 | −15.1 | 409 | PH:14/02 [06:55] | 123 | – | – | 17/02 [10:00] |
| 26 | 10/03/98 – 20:00 | −116 | −14.8 | 529 | – | – | – | – | m |
| 27 | 21/03/98 – 15:00 | −85 | −12.4 | 429 | PH:18/03 [07:33] | 413 | – | – | m |
| 28 | 25/03/98 – 16:00 | −56 | −7.2 | 401 | – | – | – | – | 25/03 [14:00] |
| 29 | 24//04/98 – 07:00 | −69 | −8.9 | 435 | FH:23/04 [05:55] | 1691 | X1.2 | – | m |
| 30 | 02/05./98 – 17:00 | −85 | −11.6 | 596 | FH:29/04 [16:58] | 1374 | M6.8 | S18E20 | 02/05 [05:00] |
| 31 | 04/05/98 – 06:00 | −205 | −28.5 | 803 | FH:01/05 [23:40] | 585 | C2.8 | N25E35 | 04/05 [10:00] |
| | | | | | FH:02/05 [05:31] | 542 | C5.4 | S20W07 | |
| | | | | | FH:02/05 [14:06] | 938 | X1.1 | S15W15 | |
| 32 | 09/05/98 – 19:00 | −63 | −5.7 | 512 | PH:06/05 [08:29] | 1099 | X2.7 | S11W65 | m |
| 33 | 14/06/98 – 11:00 | −55 | −11.1 | 325 | – | – | – | – | 14/06 [04:00] |
| 34 | 26/06/98 – 03:00 | −101 | −13 | 465 | PH:21/06 [05:35] | 192 | – | N15W30 | 26/06 [04:00] |
| 35 | 16/07/98 – 15:00 | −58 | −10.6 | 578 | dg | dg | – | – | |
| 36 | 06/08/98 – 10:00 | −138 | −19.3 | 398 | dg | dg | – | – | |
| 37 | 07/08/98 – 05:00 | −108 | −11.3 | | dg | dg | – | – | |
| 38 | 20/08/98 – 20:00 | −67 | −10.2 | 342 | dg | dg | – | – | |
| 39 | 27/08/98 – 08:00 | −155 | −14.2 | 635 | dg | dg | – | – | |
| 40 | 25/09/98 – 07:00 | −207 | −17.9 | 797 | dg | dg | – | – | |
| 41 | 01/10/98 – 01:00 | −58 | −8.4 | 472 | dg | dg | – | – | |
| 42 | 7/10/98 – 22:00 | −70 | −10.5 | 580 | dg | dg | – | – | |
| 43 | 19/10/98 – 15:00 | −112 | −16.7 | 388 | FH:15/10 [10:04] | 262 | – | – | 19/10 [04:00] |
| 44 | 22/10/98 – 18:00 | −53 | −4 | 594 | – | – | – | – | 23/10 [15:00] |
| 45 | 08/11/1998 | −149 | −19.9 | 623 | FH:04/11 [07:54] | 523 | C1.6 | N17W01 | 07/11 [22:00] |
| | | | | | FH:05/11 [20:44] | 1118 | M8.4 | N22W18 | |
| 46 | 09/11/1998 | −142 | −15.2 | 436 | FH:05/11 [20:44] | 1118 | M8.4 | N22W18 | 09/11 [01:00] |
| | | | | | PH:06/11 [02:18] | 405 | C4.4 | N19W24 | |
| 47 | 13/11/98 – 18:00 | −131 | −17 | 360 | PH:10/11 [06:18] | 286 | C3.3 | N21W64 | 13/11 [02:00] |
| 48 | 11/12/98 – 15:00 | −69 | −12.7 | 344 | PH:10/12 [23:30] | 591 | B9.3 | S22W51 | m |
| 49 | 28/12/98 – 11:00 | −58 | −6.9 | 404 | dg | – | – | – | – |
| *Year 1999* | | | | | | | | | |
| 50 | 13/01/99 – 23:00 | −112 | −14.6 | 418 | dg | – | – | – | |
| 51 | 23/01/99 – 22:00 | −52 | −4.9 | 541 | dg | – | – | – | – |
| 52 | 18/02/99 – 09:00 | −123 | −21.8 | 635 | PH:14/02 [11:08] | 758 | M1.0 | N17E05 | |
| 53 | 01/03/99 – 19:00 | −95 | −15.1 | 456 | – | – | – | – | m |

**Table 1** (*continued*)

| E. No. | Storm time | *Dst* min. (nT) | Bz (nT) | Vsw (km/s) | CME /Time | V_cmes | XRFs | XRF_Loc. | ICME /start |
|---|---|---|---|---|---|---|---|---|---|
| 54 | 10/03/99 – 08:00 | −81 | −9.5 | 429 | – | – | – | – | – |
| 55 | 17/04/99 – 07:00 | −91 | −14 | 415 | PH:13/04 [03:30] | 291 | – | – | 16/04 [18:00] |
| 56 | 31/07/99 – 01:00 | −53 | −10.6 | 625 | FH:28/07 [09:06] | 462 | – | – | 30/07 [20:00] |
| 57 | 23/08/99 – 00:00 | −66 | −9.2 | 428 | PH:20/08 [13:26] | 209 | M1.8 | S28E76 | 20/08 [23:00] |
| 58 | 13/09/99 – 04:00 | −74 | −7.4 | 566 | PH:12/09 [00:54] | 732 | B9.9 | – | m |
| 59 | 16/09/99 – 08:00 | −67 | −6.1 | 579 | PH:13/09 [09:30] | 898 | C4.9 | N22E10 | m |
| | | | | | PH:13/09 [17:31] | 444 | C2.1 | N17E75 | |
| 60 | 22/09/99 – 23:00 | −173 | −15.8 | 588 | FH:20/09 [06:06] | 604 | C2.8 | S21W05 | 22/09 [19:00] |
| 61 | 27/09/99 – 18:00 | −64 | −5.9 | 638 | – | – | – | – | m |
| 62 | 10/10/99 – 18:00 | −67 | −8.6 | 514 | – | – | – | – | m |
| 63 | 15/10/99 – 05:00 | −67 | −5.1 | 710 | FH:14/10 [09:26] | 1250 | X1.8 | N11E32 | m |
| 64 | 22/10/99 – 06:00 | −237 | −30.7 | 548 | PH:18/10 [00:06] | 144 | – | – | 21/10 [08:00] |
| | | | | | PH:19/10 [05:30] | 753 | C2.9 | – | |
| 65 | 27/10/99 – 16:00 | −66 | −6.4 | 390 | – | – | – | – | m |
| 66 | 08/11/99 – 14:00 | −73 | −7.2 | 560 | PH:05/11 [18:26] | 378 | M3.0 | S19W45 | m |
| 67 | 13/11/99 – 22:00 | −106 | −11.5 | 443 | dg | – | – | – | 13/11 [20:00] |
| 68 | 13/12/99 – 09:00 | −85 | −9.7 | 487 | dg | – | – | – | 12/12 [19:00] |
| *Year 2000* | | | | | | | | | |
| 69 | 11/01/00 – 21:00 | −81 | −15.1 | 524 | – | – | – | – | m |
| 70 | 22/01/00 – 03:00 | −97 | −15.7 | 388 | FH:18/01 [17:04] | 739 | M3.4 | S19E11 | 22/101 [17;00] |
| 71 | 12/02/00 – 11:00 | −133 | −16.4 | 568 | FH:08/02 [09:30] | 1079 | M1.3 | N25E26 | 12/02 [12:00] |
| | | | | | FH:09/02 [19:54] | 910 | C7.4 | S17W40 | |
| 72 | 31/03/00 – 11:00 | −60 | −7.2 | 396 | FH:29/03 [10:54] | 949 | C1.8 | S17E75 | 29/03 [19:00] |
| 73 | 05/04/00 – 01:00 | −63 | −7.6 | 376 | – | – | – | – | m |
| 74 | 07/04/00 – 00:00 | −288 | −27.3 | 571 | FH:04/04 [16:32] | 1188 | C9.7 | N16W66 | 07/04 [06:00] |
| 75 | 16/04/00 – 11:00 | −79 | −8.2 | 393 | – | – | – | – | m |
| 76 | 24/04/00 – 14:00 | −61 | −11 | 480 | FH:23/04 [12:54] | 1187 | – | – | 24/04 [04:00] |
| 77 | 17/05/00 – 05:00 | −92 | −9.4 | 505 | PH:15/05 [08:50] | 1549 | M4.4 | N21E75 | 16/05 [23:00] |
| | | | | | PH:15/05 [16:26] | 1212 | M1.1 | N21E73 | |
| 78 | 24/05/00 – 08:00 | −147 | −19.2 | 642 | FH:22/05 [01:50] | 649 | C6.3 | N20W22 | 24/05 [12:00] |
| 79 | 08/06/00 – 19:00 | −90 | −6.9 | 760 | FH:06/06 [15:54] | 1119 | X2.3 | N20E18 | 08/06 [12:00] |
| 80 | 26/06/00 – 17:00 | −76 | −9.2 | 540 | PH:23/06 [14:54] | 847 | M3.0 | N26W72 | 26/06 [12:00] |
| | | | | | PH:25/06 [07:54] | 1617 | M1.9 | N16W55 | |
| 81 | 16/07/00 – 00:00 | −301 | −49.4 | 1030 | FH:14/07 [10:54] | 1674 | X5.7 | N22W07 | 15/07 [19:00] |
| 82 | 20/07/00 – 09:00 | −93 | −7.9 | 563 | – | – | – | – | 20/07 [01:00] |
| 83 | 23/07/00 – 22:00 | −68 | −10.2 | 379 | PH:22/07 [11:54] | 1230 | M3.7 | N14W56 | 23/07 [15:00] |
| 84 | 29/07/00 – 11:00 | −71 | −10 | 458 | FH:25/07 [03:30] | 528 | M8.0 | N06W08 | 28/07 [12:00] |
| 85 | 06/08/00 – 05:00 | −56 | −3.7 | 553 | – | – | – | – | m |
| 86 | 11/08/00 – 06:00 | −106 | −13.2 | 426 | PH:08/08 [15:54] | 867 | C1.4 | – | 10/08 [19:00] |
| 87 | 12/08/00 – 09:00 | −235 | −28.7 | 613 | FH:09/08 [16:30] | 702 | C2.3 | N11W11 | 12/08 [05:00] |
| 88 | 29/08/00 – 06:00 | −60 | −6 | 602 | PH:25/08 [14:54] | 518 | M1.4 | S15E67 | m |
| | | | | | PH:26/08 [21:30] | 326 | C3.8 | N26E02 | |
| 89 | 02/09/00 – 14:00 | −57 | −6.6 | 444 | – | – | – | – | 02/09 [19:00] |
| 90 | 12/09/00 – 19:00 | −73 | −9.5 | 395 | PH:09/09/ [08:56] | 554 | M1.6 | N07W67 | m |
| 91 | 16/09/00 – 23:00 | −68 | −15.9 | 401 | FH:12/09 [11:54] | 1550 | M1.0 | S17W09 | m |
| 92 | 18/09/00 – 23:00 | −201 | −23.9 | 794 | FH:15/09 [21:50] | 257 | C7.4 | N12E04 | 17/09 [21:00] |
| | | | | | FH:16/09 [05:18] | 1215 | M5.9 | N14W07 | |
| 93 | 26/09/00 – 02:00 | −55 | −5.6 | 568 | – | – | – | – | m |
| 94 | 30/09/00 – 14:00 | −76 | −11.5 | 408 | FH:25/09 [02:50] | 587 | M1.8 | S11W58 | m |
| 95 | 05/10/00 – 13:00 | −182 | −20.2 | 523 | FH:02/10 [03:50] | 525 | – | – | 03/10 [10:00] |
| | | | | | FH:02/10 [20:26] | 569 | C8.4 | N01E80 | |
| 96 | 14/10/00 – 14:00 | −107 | −11.5 | 413 | FH:09/10 [23:50] | 798 | C6.7 | N01W14 | 13/10 [16:00] |
| 97 | 29/10/00 – 03:00 | −127 | −17.1 | 403 | FH:25/10 [08:26] | 770 | C4.0 | N06W60 | 28/10 [21:00] |
| 98 | 06/11/2000 – [21:00] | −159 | −11.7 | 570 | FH:03/11 [18:26] | 291 | C3.2 | N02W02 | 06/11 [17:00] |
| 99 | 10/11/00 – 12:00 | −96 | −8 | 881 | – | – | – | – | m |
| 100 | 27/11/00 – 01:00 | −80 | −10.8 | 517 | FH:24/11 [15:30] | 1245 | X2.3 | N22W07 | 27/11 [08:00] |
| | | | | | FH:24/11 [22:06] | 1005 | X1.8 | N21W14 | |
| 101 | 29/11/00 – 13:00 | −119 | −10.3 | 486 | FH:25/11 [09:30] | 675 | M8.2 | N18W24 | 28/11 [11:00] |
| | | | | | FH:25/11 [17:31] | 671 | M3.5 | N20W23 | |
| | | | | | FH:26/11 [17:06] | 980 | X4.0 | N18W38 | |
| 102 | 23/12/00 – 04:00 | −62 | −13.9 | 323 | PH:20/12 [10:30] | 1076 | – | – | 23/12 [00:00] |
| | | | | | PH:20/12 [21:30] | 609 | C3.5 | S10E48 | |

(*continued on next page*)

**Table 1** (*continued*)

| E. No. | Storm time | *Dst* min. (nT) | Bz (nT) | Vsw (km/s) | CME /Time | V_cmes | XRFs | XRF_Loc. | ICME /start |
|---|---|---|---|---|---|---|---|---|---|
| *Year 2001* | | | | | | | | | |
| 103 | 24/01/01 – 18:00 | −61 | −6.8 | 436 | FH:20/01 [19:31] | 839 | M1.2 | S07E40 | 24/01 [09:00] |
| | | | | | FH:20/01 [21:30] | 1507 | M7.7 | S07E46 | |
| 104 | 05/03/01 – 02:00 | −73 | −12.5 | 435 | PH:01/03 [18:26] | 631 | C1.2 | S09W27 | 04/03 [04:00] |
| 105 | 20/03/01 – 13:00 | −149 | −18.8 | 388 | FH:16/03 [03:50] | 389 | – | – | 19/03 [17:00] |
| 106 | 23/03/01 – 16:00 | −75 | −7.5 | 413 | PH:20/03 [03:26] | 478 | – | – | m |
| 107 | 28/03/01 – 15:00 | −87 | −6.8 | 606 | FH:24/03 [20:50] | 906 | M1.7 | N15E22 | 27/03 [20:00] |
| | | | | | FH:25/03 [17:06] | 677 | C9.0 | N16E25 | |
| 108 | 31/03/01 – 08:00 | −387 | −44.7 | 644 | FH:28/03 [12:50] | 519 | M4.3 | N18E02 | 31/03 [05:00] |
| | | | | | FH:29/03 [10:26] | 942 | X1.7 | N20W19 | |
| 109 | 04/04/01 – 07:00 | −50 | −5.5 | 645 | PH:02/04 [22:06] | 2505 | X20.0 | – | 04/04 [18:00] |
| 110 | 09/04/01 – 06:00 | −63 | −4.7 | 644 | FH:05/04 [17:06] | 1390 | M5.1 | S24E50 | 08/04 [14:00] |
| | | | | | FH:06/04 [19:30] | 1270 | X5.6 | S21E31 | |
| 111 | 11/04/01 – 23:00 | −271 | −20.5 | 725 | FH:09/04 [15:54] | 1192 | M7.9 | S21W04 | 11/04 [22:00] |
| | | | | | FH:10/04 [05:30] | 2411 | X2.3 | S23W09 | |
| 112 | 18/04/01 – 06:00 | −114 | −19.6 | 512 | PH:15/04 [14:06] | 1199 | X14.4 | S20W85 | 18/04 [12:00] |
| 113 | 22/04/01 – 15:00 | −102 | −12.8 | 351 | – | – | – | – | 21/04 [23:00] |
| 114 | 10/05/01 – 03:00 | −76 | −8.4 | 426 | PH:07/05 [12:06] | 1223 | C3.9 | N25W35 | 09/05 [12:00] |
| 115 | 18/06/01 – 08:00 | −61 | −11.6 | 363 | FH:15/06 [15:56] | 1701 | C2.2 | S16E18 | m |
| 116 | 17/08/01 – 21:00 | −105 | −18.1 | 519 | FH:14/08 [16:01] | 618 | C2.3 | N16W36 | 17/08 [20:00 |
| 117 | 13/09/01 – 07:00 | −57 | −7.2 | 395 | FH:11/09 [14:54] | 791 | C3.2 | N13E35 | 13/09 [18:00] |
| 118 | 23/09/01 – 18:00 | −73 | −9 | 525 | PH:20/09 [19:31] | 446 | C3.2 | S17E54 | 24/09 [00:00] |
| 119 | 26/09/01 – 01:00 | −102 | −6.4 | 627 | FH:24/09 [10:30] | 2402 | X2.6 | S16E23 | m |
| 120 | 01/10/01 – 08:00 | −148 | −12.7 | 481 | FH:28/09 [08:54] | 846 | M3.3 | N10E182N | 01/10 [08:00] |
| 121 | 03/10/01 – 14:00 | −166 | −20.9 | 520 | PH:09/29 [11:54] | 509 | M1.8 | N13E03 | 02/10 [04:00] |
| 122 | 12/10/01 – 12:00 | −71 | −13.2 | 479 | FH:09/10 [11:30] | 973 | M1.4 | S28E08 | 12/10 [04;00] |
| 123 | 19/10/01 – 21:00 | −57 | −7.4 | 340 | – | – | – | – | m |
| 124 | 21/10/01 – 21:00 | −187 | −16.4 | 608 | FH:19/10 [01:27] | 558 | X1.6 | N16W18 | 21/10 [20:00] |
| | | | | | FH:19/10 [16:50] | 901 | X1.6 | N15W29 | |
| 125 | 28/10/01 – 11:00 | −157 | −14.5 | 474 | FH:25/10 [15:26] | 1092 | X1.3 | S16W21 | 29/10 [22:00] |
| 126 | 01/11/01 – 10:00 | −106 | −13 | 348 | – | – | – | – | 31/10 [20:00] |
| 127 | 06/11/01 – 06:00 | −292 | −64 | 729 | FH:03/11 [19:20] | 457 | – | – | 05/11 [19:00] |
| | | | | | FH:04/11 [16:35] | 1810 | X1.0 | N06W18 | |
| 128 | 24/11/01 – 16:00 | −221 | −27.8 | 1034 | FH:21/11 [14:06] | 518 | C4.7 | S14W19 | 24/11 [14:00] |
| | | | | | FH:22/11 [20:30] | 1443 | M3.8 | S25W67 | |
| | | | | | FH:22/11 [23:30] | 1437 | M9.9 | S14W36 | |
| 129 | 21/12/01 – 22:00 | −67 | −9.1 | 423 | – | – | – | – | m |
| 130 | 30/12/01 – 05:00 | −58 | −9.7 | 382 | PH:26/12 [05:30] | 1446 | M7.1 | N08W54 | 30/12 [00:00] |
| *Year 2002* | | | | | | | | | |
| 131 | 11/01/02 – 06:00 | −72 | −4.5 | 630 | FH:08/01 [17:54] | 1794 | C7.2 | S18W42 | m |
| 132 | 02/02/02 – 09:00 | −86 | −12.7 | 370 | – | – | – | – | m |
| 133 | 05/02/02 – 20:00 | −82 | −7.7 | 523 | PH:02/02 [15:54] | 362 | C2.2 | S18W13 | m |
| 134 | 01/03/02 – 01:00 | −71 | −14.6 | 390 | – | – | – | – | 28/02 [17:00] |
| 135 | 24/03/02 – 09:00 | −100 | −9.4 | 421 | FH:20/03 [17:54] | 603 | C4.0 | S21W15 | 24/03 [12:00] |
| | | | | | PH:19/03 [11:54] | 860 | M1 | S10W58 | |
| 136 | 18/04/02 – 07:00 | −127 | −12.8 | 504 | FH:15/04 [03:50] | 720 | M1.2 | S15W01 | 17/04 [16:00] |
| 137 | 20/04/02 – 08:00 | −149 | −14.7 | 611 | FH:17/04 [08:26] | 1240 | M2.6 | S14W34 | 20/04 [00:00] |
| 138 | 11/05/02 – 19:00 | −110 | −16.5 | 437 | FH:08/05 [13:50] | 614 | C4.2 | S12W07 | 11/05 [15:00] |
| 139 | 15/05/02 – 00:00 | −65 | −6.8 | 412 | – | – | – | – | m |
| 140 | 23/05/02 – 17:00 | −109 | −14.1 | 871 | FH:22/05 [03:50] | 1557 | C5.0 | S22W53 | 23/05 [20:00] |
| 141 | 27/05/02 – 09:00 | −64 | −12 | 553 | PH:25/05 [02:50] | 880 | C1.7 | S18W13 | m |
| 142 | 02/08/02 – 05:00 | −102 | −12.5 | 524 | PH:29/07 [12:07] | 562 | – | – | 01/08 [09:00] |
| | | | | | PH:01/08 [04:06] | 375 | C2.5 | S10E12 | |
| 143 | 21/08/02 – 02:00 | −106 | −9.2 | 434 | FH:16/08 [12:30] | 1585 | M5.2 | S14E20 | 19/08 [12:00] |
| 144 | 04/09/02 – 05:00 | −109 | −18.3 | 514 | – | – | – | | m |
| 145 | 08/09/02 – 00:00 | −181 | −21.5 | 520 | FH:05/09 [16:54] | 1748 | C5.2 | N09E28 | 08/09 [04:00] |
| | | | | | FH:06/09 [13:31] | 909 | C2.0 | NA | |
| 146 | 01/10/02 – 16:00 | −176 | −21.8 | 379 | PH:09/30 [01:31] | 307 | M2.1 | N13E10 | 30/09 [20:00] |
| 147 | 04/10/02 – 08:00 | −146 | −11.8 | 388 | PH:02/10 [07:31] | 903 | B9.2 | S18E20 | 03/10 [01:00] |
| 148 | 07/10/02 – 07:00 | −115 | −8.4 | 371 | PH:04/10 [20:30] | 743 | C4.8 | N12E46 | – |
| 149 | 14/10/02 – 13:00 | −100 | −13.6 | 355 | – | | – | – | m |
| 150 | 24/10/02 – 19:00 | −94 | −7.4 | 732 | – | – | – | – | m |

**Table 1** (*continued*)

| E. No. | Storm time | *Dst* min. (nT) | Bz (nT) | Vsw (km/s) | CME /Time | V_cmes | XRFs | XRF_Loc. | ICME /start |
|---|---|---|---|---|---|---|---|---|---|
| 151 | 27/10/02 – 16:00 | −65 | −4.3 | 608 | – | – | – | – | m |
| 152 | 31/10/02 – 18:00 | −52 | −5.3 | 437 | FH:27/10 [23:18] | 2115 | – | – | m |
| 153 | 3/11/2002 – 06:00 | −75 | −6.3 | 480 | – | – | – | – | m |
| 154 | 18/11/02 – 22:00 | −52 | −7.7 | 379 | FH:16/11 [07:12] | 1185 | C1.9 | S19W18 | 17/11 [10:00] |
| 155 | 21/11/02 – 10:00 | −128 | −13.1 | 656 | – | – | – | – | m |
| 156 | 27/11/02 – 06:00 | −64 | −4.8 | 544 | FH:24/11 [20:30] | 1077 | C6.4 | S17W37 | m |
| 157 | 21/12/02 – 03:00 | −75 | −8.1 | 495 | – | – | | | 21/12 [23:00] |
| 158 | 23/12/02 – 11:00 | −67 | −5.6 | 581 | FH:19/12 [22:06] | 1092 | M2.7 | N15W08 | m |
| 159 | 27/12/02 – 04:00 | −68 | −8.1 | 638 | – | – | – | – | m |
| *Year 2003* | | | | | | | | | |
| 160 | 30/01/03 – 00:00 | −66 | −8.8 | 438 | PH:27/01 [22:23] | 1053 | C2.4 | S17W23 | m |
| 161 | 04/02/03 – 09:00 | −74 | −8.2 | 593 | PH:30/01 [10:06] | 325 | B4.8 | S11E52 | 01/02 [19:00] |
| 162 | 27/02/03 – 21:00 | −66 | −5.8 | 509 | – | – | – | – | m |
| 163 | 04/03/03 – 07:00 | −67 | −12.4 | 524 | – | – | – | – | m |
| 164 | 16/03/03 – 21:00 | −60 | −6.1 | 685 | PH:14/03 [18:06] | 991 | B9.2 | S20W66 | m |
| 165 | 20/03/03 – 19:00 | −64 | −7.3 | 645 | FH:19/03 [02:30] | 1342 | M1.5 | S15W54 | 20/03 [12:00] |
| 166 | 04/04/03 – 23:00 | −62 | −6.5 | 478 | – | – | – | – | m |
| 167 | 01/05/03 – 00:00 | −78 | −8.1 | 634 | – | – | – | – | m |
| 168 | 10/05/03 – 08:00 | −84 | −7.4 | 625 | – | – | – | – | 09/05 [07:00] |
| 169 | 22/05/03 – 02:00 | −73 | −10.2 | 522 | – | – | – | – | m |
| 170 | 29/05/03 – 23:00 | −144 | −12.7 | 737 | FH:27/05 [06:50] | 509 | M1.6 | S07W14 | 29/05 [13:00] |
| | | | | | FH:28/05 [00:50] | 1366 | X3.6 | S11W11 | |
| | | | | | FH:27/05 [23:50] | 964 | X1.3 | S07W17 | |
| 171 | 02/06/03 – 08:00 | −91 | −8.9 | 716 | FH:31/05 [02:30] | 1835 | M9.3 | S07W65 | m |
| 172 | 18/06/03 – 09:00 | −141 | −16.7 | 524 | FH:15/06 [23:54] | 2053 | X1.3 | S07E80 | 17/06 [10:00] |
| | | | | | PH:14/06 [05:30] | 1215 | M1.5 | S06E89 | |
| 173 | 12/07/03 – 05:00 | −105 | −13.2 | 589 | – | – | – | – | m |
| 174 | 16/07/03 – 13:00 | −90 | −10.4 | 569 | – | – | – | – | m |
| 175 | 06/08/03 – 06:00 | −60 | −11 | 483 | – | – | – | – | 04/08 [22:00] |
| 176 | 07/08/03 – 21:00 | −61 | −9.5 | 601 | FH:03/08 [00:30] | 699 | M1.3 | S17E63 | m |
| 177 | 18/08/03 – 15:00 | −148 | −15.9 | 437 | FH:14/08 [20:06] | 378 | – | S30E00 | 18/08 [01:00] |
| 178 | 21/08/03 – 06:00 | −68 | −4.6 | 568 | – | – | – | – | m |
| 179 | 17/09/03 – 23:00 | −65 | −6.2 | 747 | – | – | – | – | m |
| 180 | 14/10/03 – 22:00 | −85 | −8.6 | 619 | – | – | – | – | m |
| 181 | 22/10/03 – 06:00 | −61 | −4.7 | 688 | FH:18/10 [15:30] | 627 | C3.3 | N07E72 | 22/10 [02:00] |
| 182 | 27/10/03 – 04:00 | −52 | −7.7 | 476 | PH:26/10 [06:54] | 1371 | X1.2 | S15E44 | 25/10 [14:00] |
| | | | | | PH:26/10 [17:54] | 1537 | X1.2 | N02W38 | |
| 183 | 30/10/03 – 22:00 | −383 | −27.1 | 1161 | FH:28/10 [11:30] | 2459 | X17.2 | S16E08 | 29/10 [11:00] |
| | | | | | FH:29/10 [20:54] | 2029 | X10.0 | S15W02 | |
| 184 | 04/11/03 – 10:00 | −69 | −11.9 | 739 | FH:02/11 [17:30] | 2598 | X8.3 | S14W56 | m |
| 184 | 11/11/03 – 13:00 | −62 | −6 | 710 | – | – | – | – | m |
| 186 | 13/11/03 – 20:00 | −59 | −3.8 | 656 | FH:11/11/ [13:54] | 1315 | M1.6 | S03W61 | m |
| 187 | 20/11/03 – 20:00 | −422 | −50.9 | 553 | FH:18/11 [08:50] | 1668 | M3.9 | N03E18 | 20/11 [10:00] |
| 188 | 06/12/2003 – 04:00 | −55 | −8 | 533 | – | – | – | – | m |
| 189 | 08/12/03 – 21:00 | −54 | −7.9 | 616 | – | – | – | – | m |
| *Year 2004* | | | | | | | | | |
| 190 | 07/01/04 – 09:00 | −69 | −6.2 | 736 | – | – | – | – | m |
| 191 | 10/01/04 – 08:00 | −60 | −7 | 551 | PH:07/01 [10:30] | 1822 | M8.3 | N06E75 | 10/01 [06:00] |
| | | | | | PH:08/01 [05:06] | 1713 | M1.3 | N03E63 | |
| 192 | 22/01/04 – 13:00 | −149 | −14.9 | 614 | FH:20/01 [0:06] | 965 | C5.5 | S13W11 | 22/01 [08:00] |
| 193 | 11/02/04 – 17:00 | −109 | −13.6 | 385 | – | – | – | – | m |
| 194 | 10/03/04 – 08:00 | −77 | −9.5 | 765 | – | – | – | – | m |
| 195 | 04/04/04 – 01:00 | −112 | −7.9 | 506 | – | – | – | – | 03/04 [14:00] |
| 196 | 05/04/04 – 19:00 | −81 | −15.7 | 419 | – | – | – | – | m |
| 197 | 17/07/04 – 02:00 | −80 | −14.1 | 468 | FH:13/07 [09:30] | 747 | M5.4 | N14W51 | m |
| 198 | 23/07/04 – 02:00 | −101 | −15.5 | 643 | FH:20/07 [13:31] | 710 | M8.6 | N10E35 | 22/07 [18:00] |
| 199 | 25/07/04 – 11:00 | −148 | −17 | 593 | PH:22/7 [08:30] | 899 | C5.3 | N02E08 | 24/07 [14:00] |
| | | | | | FH:23/07 [16:06] | 824 | C1.0 | N05W04 | |
| 200 | 27/07/04 – 13:00 | −197 | −19.9 | 831 | FH:25/07 [14:54] | 1333 | M1.1 | N08W33 | 27/07 [02:00] |
| 201 | 30/08/04 – 22:00 | −126 | −14.3 | 416 | – | – | – | – | 29/08 [19:00] |
| 202 | 14/09/04 – 11:00 | −50 | −5.5 | 580 | FH:12/09 [00:36] | 1328 | M4.8 | N03E49 | 14/09 [15:00] |
| 203 | 13/10/04 – 13:00 | −63 | −8.6 | 470 | – | – | – | – | m |

(*continued on next page*)

**Table 1** (*continued*)

| E. No. | Storm time | *Dst* min. (nT) | Bz (nT) | Vsw (km/s) | CME /Time | V_cmes | XRFs | XRF_Loc. | ICME /start |
|---|---|---|---|---|---|---|---|---|---|
| 204 | 08/11/04 – 06:00 | −373 | −44.9 | 712 | FH:04/11 [09:54] | 653 | C6.3 | N09E28 | 07/11 [22:00] |
| | | | | | FH:06/11 [01:31] | 818 | M3.6 | N10E06 | |
| 205 | 12/11/04 – 10:00 | −109 | −3.8 | 588 | FH:07/11 [16:54] | 1759 | X2.0 | N09W17 | 12/11 [08:00] |
| | | | | | FH:10/11 [02:26] | 3387 | X2.5 | N09W49 | |
| 206 | 21/11/04 – 11:00 | −60 | −3.5 | 601 | – | – | – | – | m |
| 207 | 25/11/04 – 07:00 | −63 | −6.8 | 498 | – | – | – | – | m |
| 208 | 06/12/04 – 15:00 | −58 | −7.8 | 439 | FH:03/12 [0:26] | 1216 | M1.5 | N08W02 | m |
| 209 | 13/12/04 – 04:00 | −61 | −9.8 | 395 | FH:08/12 [20:26] | 611 | M1.2 | S08E66 | 12/12 [22:00] |
| 210 | 29/12/04 – 10:00 | −55 | −7.6 | 420 | – | – | – | – | m |
| *Year 2005* | | | | | | | | | |
| 211 | 01/01/05 – 19:00 | −57 | −9.4 | 459 | FH:30/12 [22:30] | 1035 | M4.2 | N04E46 | m |
| 212 | 08/01/05 – 02:00 | −96 | −18.5 | 548 | – | – | – | – | 08/01 [22:00] |
| 213 | 12/01/05 – 10:00 | −57 | −10.9 | 598 | PH: 09/01 [09:06] | 870 | M2.4 | S09E70 | m |
| 214 | 18/01/05 – 08:00 | −121 | −15.5 | 957 | FH:15/01 [06:30] | 2049 | M8.6 | N16E04 | 18/01 [23:00] |
| | | | | | FH:15/01 [23:06] | 2861 | X2.6 | N15W05 | |
| 215 | 22/01/05 – 06:00 | −105 | −6.3 | 814 | FH:19/01 [08:29] | 2020 | X1.3 | N15W51 | 21/01 [19:00] |
| | | | | | FH:20/01 [06:54] | 882 | X7.1 | N14W61 | |
| 216 | 07/02/05 – 21:00 | −62 | −6.6 | 682 | – | – | – | – | 216 |
| 217 | 18/02/05 – 02:00 | −86 | −15.9 | 436 | – | – | – | – | 18/02 [14:00] |
| 218 | 06/03/05 – 16:00 | −65 | −6.5 | 610 | – | – | – | – | m |
| 219 | 05/04/05 – 05:00 | −85 | −6.5 | 689 | – | – | – | – | m |
| 220 | 12/04/05 – 05:00 | −70 | −8.5 | 492 | PH:09/04 [08:26] | 329 | B2.6 | S07W63 | m |
| | | | | | PH:09/04 [13:50] | 514 | B2.1 | S07W66 | |
| 221 | 08/05/05 – 18:00 | −127 | −13 | 755 | FH:05/05 [20:30] | 1180 | C7.8 | S04W67 | m |
| 222 | 15/05/05 – 08:00 | −263 | −38 | 835 | FH:11/05 [20:13] | 550 | M1.1 | S11W51 | 15/05 [06:00] |
| | | | | | FH:13/05 [17:12] | 1689 | M8.0 | N12E11 | |
| 223 | 20/05/05 – 08:00 | −103 | −9.1 | 478 | PH:16/05 [13:50] | 405 | C1.2 | N13W29 | 20/05 [03:00] |
| | | | | | PH:17/05 [03:26] | 449 | M1.8 | S15W00 | |
| 224 | 30/05/05 – 13:00 | −138 | −161 | 451 | FH:26/05 [15:06] | 586 | B7.5 | S12E13 | 30/05 [01:00] |
| 225 | 13/06/05 – 00:00 | −106 | −16.8 | 464 | PH:09/06 [14:36] | 377 | C1.3 | N07E13 | 12/06 [15:00] |
| 226 | 15/06/05 – 12:00 | −54 | −6.9 | 507 | – | – | – | – | 15/06 [05:00] |
| 227 | 23/06/05 – 10:00 | −97 | −17.2 | 385 | – | – | – | – | m |
| 228 | 09/07/05 – 18:00 | −60 | −9.2 | 338 | FH:05/07 [15:30] | 772 | C1.3 | S08E34 | m |
| 229 | 10/07/05 – 20:00 | −94 | −19.2 | 438 | FH:09/07 [22:30] | 1540 | M2.8 | N12W28 | 10/07 [10:00] |
| 230 | 18/07/05 – 06:00 | −76 | −8.8 | 418 | FH:14/07 [10:54] | 2115 | X1.2 | N11W90 | 17/07 [17:00] |
| 231 | 10/08/05 – 11:00 | −53 | −8.7 | 433 | – | – | – | – | 10/08 [06:00] |
| 232 | 24/08/05 – 11:00 | −216 | −38.3 | 620 | FH:22/08 [01:31] | 1194 | M2.6 | S11W54 | 24/08 [14;00] |
| | | | | | FH:22/08 [17:30] | 2378 | M5.6 | S13W65 | |
| 233 | 31/08/05 – 19:00 | −131 | −15.8 | 415 | – | – | – | – | m |
| 234 | 11/09/05 – 09:00 | −147 | −8.5 | 974 | FH:09/09 [19:48] | 2257 | X6.2 | S12E67 | 11/09 [05:00] |
| 235 | 15/09/05 – 16:00 | −86 | −4.8 | 862 | FH:13/09 [20:00] | 1866 | X1.5 | S09E10 | 15/09 [06:00] |
| 236 | 31/10/05 – 19:00 | −75 | −8.9 | 361 | – | – | – | – | 31/10 [02:00] |
| *Year 2006* | | | | | | | | | |
| 237 | 05/04/06 – 15:00 | −87 | −12.2 | 380 | – | – | – | – | m |
| 238 | 09/04/06 – 07:00 | −80 | −15.5 | 437 | – | – | – | – | m |
| 239 | 14/04/06 – 09:00 | −111 | −14.2 | 518 | PH:10/04 [06:06] | 184 | B4.4 | S12W22 | 14/04 [13:00] |
| 240 | 19/08/06 – 21:00 | −71 | −11.5 | 405 | FH:16/08 [16:30] | 888 | – | – | 20/08 [13:00] |
| 241 | 24/09/06 – 09:00 | −56 | −7.4 | 656 | – | – | – | – | m |
| 242 | 10/11/06 – 06:00 | −51 | −12.5 | 471 | FH:06/11 [17:54] | 1994 | C8.8 | N00E89 | m |
| 243 | 30/11/06 – 13:00 | −74 | −9.8 | 412 | – | – | – | – | 29/11 [05:00] |
| 244 | 15/12/06 – 07:00 | −146 | −14.7 | 737 | FH:13/12 [02:54] | 1774 | X3.4 | S06W23 | 14/12 [22:00] |

in 0.1–0.8 nm band. X and M flares are the most powerful with M-class intensity ranging between $10^{-5} \leqslant I \leqslant 10^{-4}$ W m$^{-2}$, while X-class intensity range is $I \geqslant 10^{-4}$ W m$^{-2}$. Various observational techniques are available to identify the surface location of CME eruptions and include for example the SOHO's Extreme-Ultraviolet Imaging Telescope (EIT). The LASCO/EIT images provide a measure of heliographic source coordinates for halo CMEs associated with flare activity. Where available, the GOES data list also provides the source coordinates of flare eruptions which have been assumed in this study to be the source location of associated geoeffective halo CMEs. Despite the assumption made for this analysis, it is important to note that this analysis did not consider various eruptive signatures (other than solar flares) at various wavelengths which may indicate the launch of a CME (Wang et al., 2011). However, the close connectivity between halo CMEs and solar flares, in addition to their

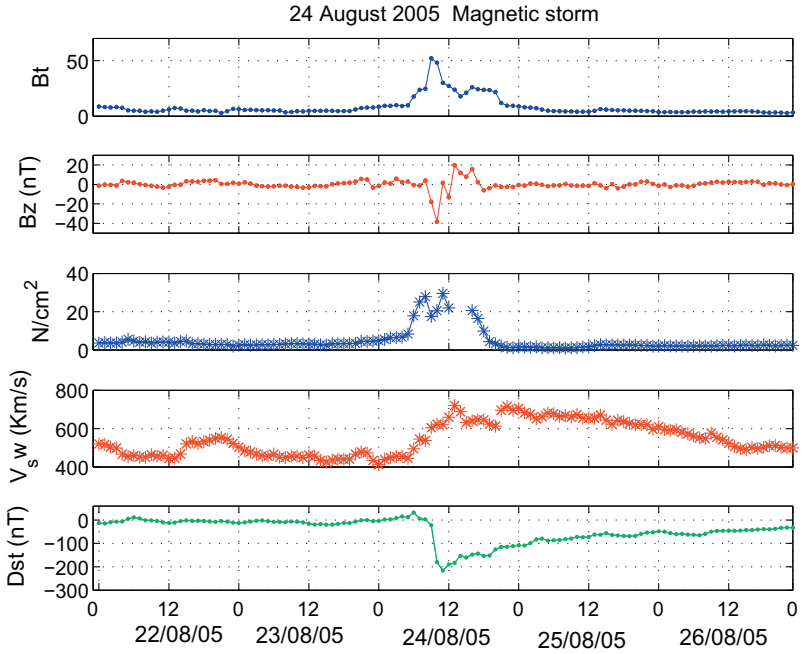


Fig. 2. Illustration of the perturbations induced in the solar wind $B_t$, $B_z$, $N$ and $V$ parameters following the arrival of an ICME. The bottom plot indicates the corresponding *Dst* index measurements for the period around the storm event of 24 August 2005.

associated IP properties can be sufficient enough for the analysis of storm efficiency. In fact, all the above mentionned parameters (AW of CMEs, solar flares, SW speed and *Bs*) have recently been shown to be suitable parameters for an empirical magnetic storms forecasting (Uwamahoro et al., 2012).

The CME data used in this study are from the LASCO/CME catalogue list (Yashiro et al., 2004). The list is generated by NASA and the Catholic University of America in collaboration with the Naval Research Laboratory and is available online at http://cdaw.gsfc.nasa.gov/CME_list. The solar flares data used are provided by the Geostationary Operational Environmental Satellite (GOES) through the Solar Geophysical Data (SGD) Center and the data can be found online on the website: http://www.ngdc.noaa.gov/stp/solar/solarflares.html.

## 3. Methods of investigation

The average transit time for CMEs to travel from the Sun to Earth is estimated at 80 h (Brueckner et al., 1998). However, this transit time does not hold during solar maximum where very fast CMEs are observed. Cane and Richardson (2003) suggested a transit time that generally ranges from 1 to 5 days. For this analysis, a 5-day time window prior to the occurrence of a storm was used to explore probable halo CMEs (and their properties) causes of the subsequent GMS. For every selected storm, the process consisted of examining the LASCO CME catalogue list to track backward in the search window for the existence of halo CME as the potential cause of the associated storm. Despite the fact that one isolated storm may be the result of more than one halo CMEs (Gopalswamy et al., 2007), all halo CMEs found in a 5-day time window were not considered as potential causes of the storm. This is due to the fact that some halo CMEs may be backsided and therefore not likely to hit the Earth. Generally, only frontside CMEs are able to reach the Earth and produce GMS although the ability of some backsided CMEs to produce minor storms has been reported in a study by (Webb et al., 2000). In this analysis, the information regarding halo CMEs association with X-ray flares has been one of the primary criteria to define a potential CME cause of the corresponding storm. However, this was only done on storm events for which the flare information was available (EIT and GOES data). The following are some examples of selected GMS events and associated solar and IP properties.

Event number 232 in Table 1 is the latest among severe GMS in SC 23. The main phase of the storm occurred on 24 August 2005 with a peak minimum *Dst* of −216 nT. The $B_s$ reached a peak value of −38.3 nT while the SW speed at the time of peak minimum *Dst* was 620 km/s. As indicated in Table 1, two high speed ($V > 1000$ km/s) full halo CMEs were considered as probable sources of the storm. The two CMEs involved were all associated with M-class solar flares and the corresponding surface coordinates are also indicated. This represents a particular example among many other multiple halo CME-driven storms.

Another example is the event number 187 in Table 1 which was the greatest among all GMS events in SC 23 occurring on 20 November 2003 at 20:00 UT (peak minimum $Dst \leqslant -422$ nT). The source of this storm was a full halo and earth-directed CME that occurred on 18 November 2003 at 08:50 UT. This very fast halo CME ($V = 1668$ km/s) was associated with an $M3.9$ class X-ray flare originating from the solar surface location at

*N*0*E*18. The storm was preceded by the presence of an ICME, first recorded on 20 November at 10:00 UT according to the catalogue of ICMEs by Richardson and Cane (2010).

Finally as shown in Table 1, 80 GMS events including few intense storms were found without any background association with halo CMEs. An example is the storm event number 195 in Table 1, which occurred on 04 April 2004 with peak minimum *Dst* of −112 nT. Such storms may be caused by CIRs or their associated effect with non halo CMEs if they arrive near Earth with a southward pointing *Bs* (Gopalswamy et al., 2007). However, the RC catalogue of ICMEs at 1 AU indicates that this storm event was associated with an ICME, starting on 03 April at 14:00 UT. This is an example of some observed cases where an ICME were detected without any link to halo CME in the 5-day time window. Such cases have also been reported in previous studies (e.g., Cane and Richardson, 2003; Richardson and Cane, 2010). The identified non-halo CME-associated storms could be the results of frontside CMEs which are not detected by SOHO spacecraft. The existence of such undetected CMEs or "SOHO stealth" CMEs has been confirmed by the STEREO twin spacecraft mission (e.g., Robbrecht et al., 2009; Wang et al., 2011 and references therein). This investigation also confirms the fact that there is no one-to-one association between ICME structure and a storm (Richardson and Cane, 2011). Storm events with or without association with ICMEs are indicated in column 10 of Table 1.

## 4. Results and discussion

A total of 244 GMS events were found over the 11-year period: 1996–2006. The period after 2006 until end of SC 23 (2009) was magnetically quiet and therefore without a particular interest for this analysis. Within the period of study, 90 (about 37%) intense GMS and 154 (about 63%) moderate GMS were investigated to determine the probable associated solar and IP properties. 15 storm events have been excluded, corresponding to the period of missing SOHO/LASCO data records, mainly in July, August and September 1998, as well as in January 1999. The missing data is indicated as data gap (*dg*) in Table 1. Therefore, the analysis concerned only 229 GMS events.

### 4.1. Intense and moderate storms

Among 229 GMS events for which the probable sources could be investigated, 84 were intense storms with an average storm strength of about $Dst = -154$ nT against 145 moderate storms with an average $Dst = -70$ nT. 70 out of the 84 intense storms (about 83%) were found to be associated with halo CMEs. As far as the 145 moderate storms are concerned, 79 of them (about 54%) were halo CME-driven storms, while the remaining 66 (about 46%) had no halo CME background in a 5-day window. The non halo CME-driven storms were assumed to be associated with

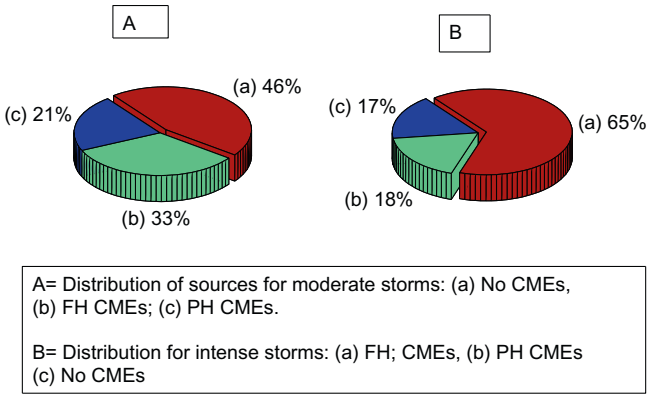


Fig. 3. Distribution of probable causes of GMS in SC 23: For moderate GMS (A): (a) represent the fraction of GMS non associated to halo CMEs (undetected CMES or CIR-driven storms), (b) the fraction of storms associated to full halo and (c) the fraction associated to partial halo CMEs. For intense storms (B): (a) represents the fraction of storms associated to full halo CMEs, while (b) and (c) represent the fraction of storms associated to partial and non halo CMEs respectively.

CIR structures originating from coronal holes (CHs) or otherwise resulting from "stealth" CMEs. The results indicate, therefore, that a large number of moderate storms have no (or undetected) halo CME background. Fig. 3 illustrates the distribution of probable sources for both moderate and intense storms in SC 23 showing the fraction of storms that were associated with full, partial and non halo CMEs respectively.

With regards to the association of GMS with ICMEs, the results obtained from this analysis show that 72 of 84 intense GMS (about 86%) were associated with ICMEs at 1 AU, compared to moderate storms for which only 44% were associated with ICMEs. Note that Table 1 contains 92 GMS events not listed in the RCs table. These events noted as *m* in column 10 are obviously among the non ICME-associated GMS and they are mostly moderate storms (81 out of 92 or 88%). The magnitude of the SW speed and $B_s$ associated with GMS were characteristics to moderate and intense storms. As illustrated in Fig. 4, intense storms were associated with higher average values of $B_s$ and SW speed compared to those for moderate storms. Table 2 presents a simplified quantitative classification of probable sources for both moderate and intense GMS during SC 23.

An investigation was carried out to quantitatively show the association of X-ray flares with the identified halo CME-driven GMS. This analysis identified 64 intense storms and 62 moderate storms cases that were clearly associated with flare activity within ±0.5 h of the corresponding probable driving CME-eruption. Table 3, provides the X-ray flare distribution per class associated to 126 CME-driven GMS events (intense and moderate storms inclusive). The data in Table 3 show that the majority of storms were associated with C and M class flares, with more than a half of all GMS (56%) linked to halo CMEs associated with powerful M and X class flares.

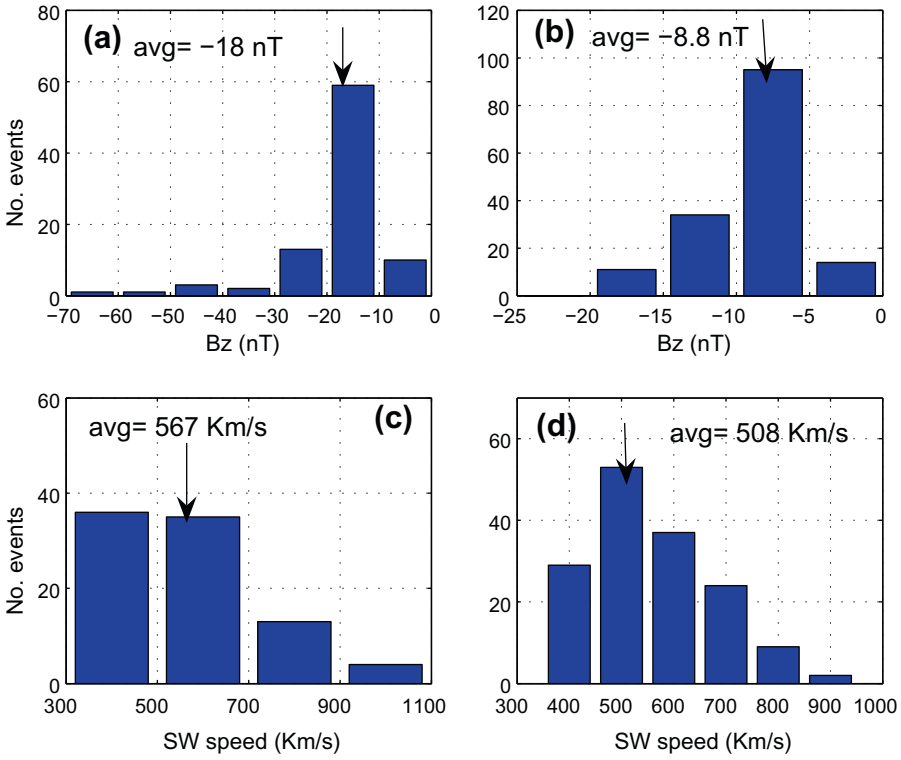


Fig. 4. Distribution of the magnitudes of *Bs* and SW speed that were associated with intense GMS in (a) and (c) as compared to those associated with moderate GMS in (b) and (d). The average values of the parameters are shown by arrows.

Table 2
Distribution of the probable sources of GMS in SC 23: Columns 3, 4, 5 indicate the percentage of storms associated with full halo (FH), partial halo (PH) and no halo CME-driven storms respectively. Column 6 shows the percentage of association with ICMEs for both intense and moderate GMS.

| Storm category | No. of GMS | FH-CME | PH-CME | No CMEs | ICMEs |
|---|---|---|---|---|---|
| Intense storms | 84 | 55 [65%] | 15 [18%] | 14 [17%] | 72 [86%] |
| Moderate storms | 145 | 48 [33%] | 31 [21%] | 66 [46%] | 64 [44%] |
| Total | 229 | 103 [45%] | 46 [20%] | 80 [35%] | 136 [59%] |

As far as solar flares surface coordinates are concerned, the solar surface flare information could be identified corresponding to 72 halo CMEs probable sources of intense GMS events. Among them, 50 events representing 69% originated close to the solar disk center [within ±45° of the central meridian distance (CMD) interval]. For moderate storms, the flaring source was available for 61 events among which only 31 of them (about 51%) were found to originate close to the disk center. These results indicate that generally intense storms were mostly associated to halo CMEs originating close to solar disc center as compared to the CMEs at the origin of moderate storms.

Table 3
Distribution of 126 solar X-ray flares per class that were associated with geoeffective halo CMEs in SC 23.

| Flare class | B-class | C-class | M-class | X-class |
|---|---|---|---|---|
| Number | 9 | 46 | 48 | 23 |
| Percentage | 7% | 37% | 38% | 18% |

### 4.2. Storm distribution over full and partial halo CMEs

As shown in Table 2, 46 events representing 31% of the total number of halo CME-driven storms (149) were uniquely associated with partial halo CMEs. In order to compare solar and IP geoeffective parameters accompanying full and partial halo CMEs, an equivalent sample of 46 full halo CME-driven GMS was selected from 1996 to 2001. Comparative results obtained show that partial halo CME-driven storms were predominantly moderate (average $Dst = -92$ nT), while intense storms with *Dst* of −128 nT on average were mainly associated with full halo CMEs. Figs. 5 and 6 compare some geoefffective parameters associated with both full and partial halo CME-driven storms, demonstrating a higher storm association with full halo than partial halo CMEs. On the other hand, this analysis shows that 42 (91%) of storms having full halo CMEs background were associated with ICMEs. For storms with partial halo background, only 71% were associated with ICMEs at 1 AU. Table 2 also shows that 80 (35%) storm

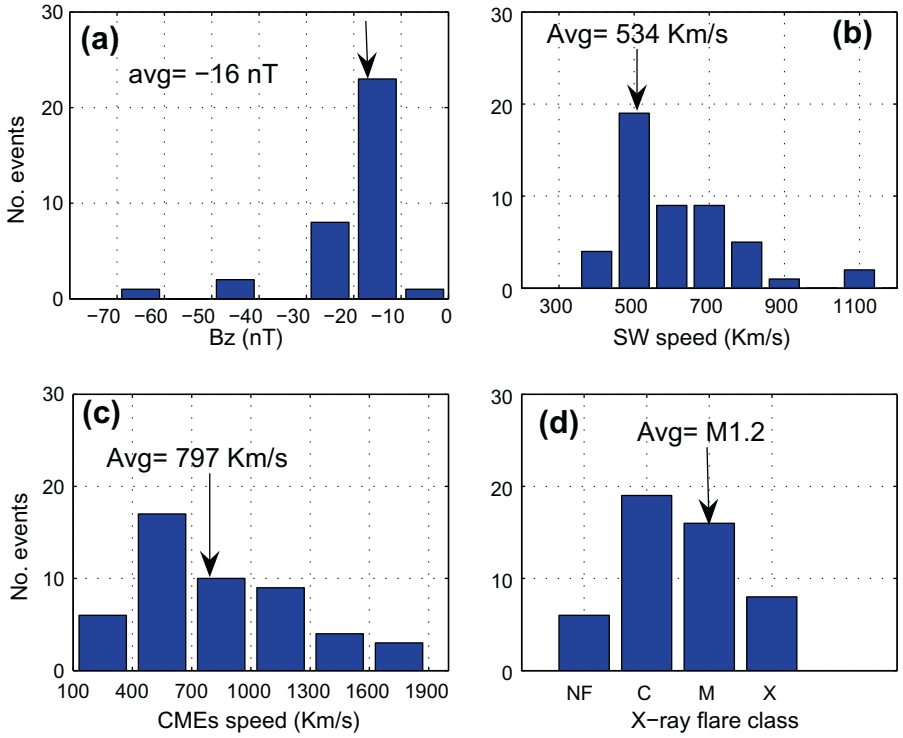


Fig. 5. Distribution of the magnitudes of *Bs*, SW speed, CMEs speed and X-ray flares that were associated with full halo CMEs.

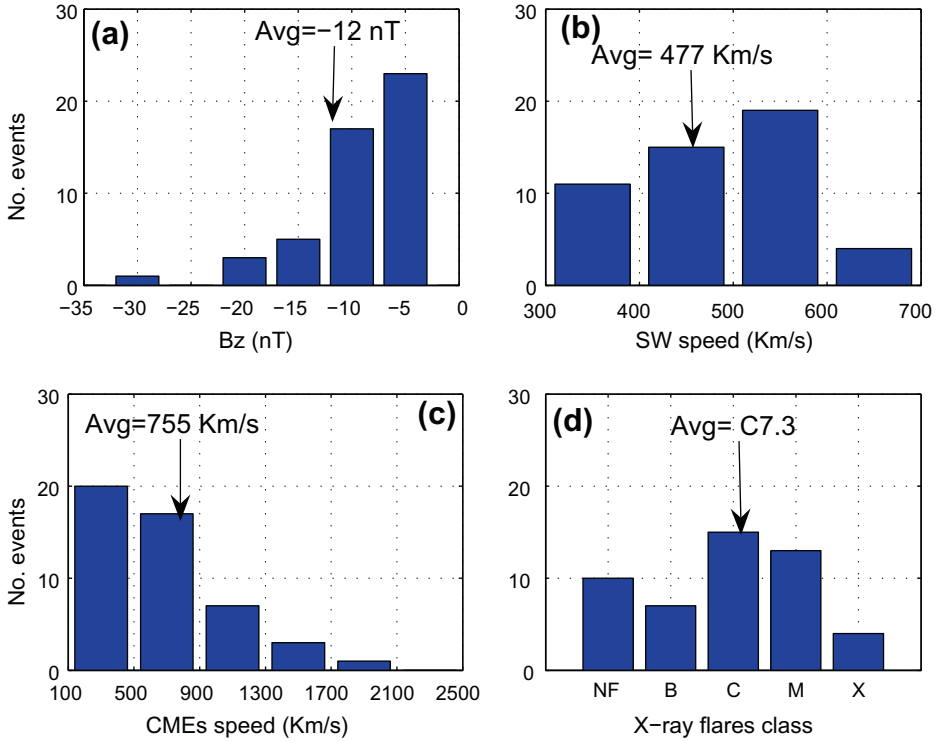


Fig. 6. Distribution of the magnitudes of *Bs*, SW speed, CMEs speed and X-ray flares that were associated with partial halo CMEs.

events were not associated with halo CMEs. However, the non halo CME-associated storms were mostly moderate storms at 88%) among which (74%) were not associated with ICMEs at 1 AU. In fact, a large number of the non halo CME-driven storms do not appear on the RCs catalogue list of ICMEs.

Figs. 5 and 6 also provide a comparative X-ray flare association between geoeffective partial and full halo

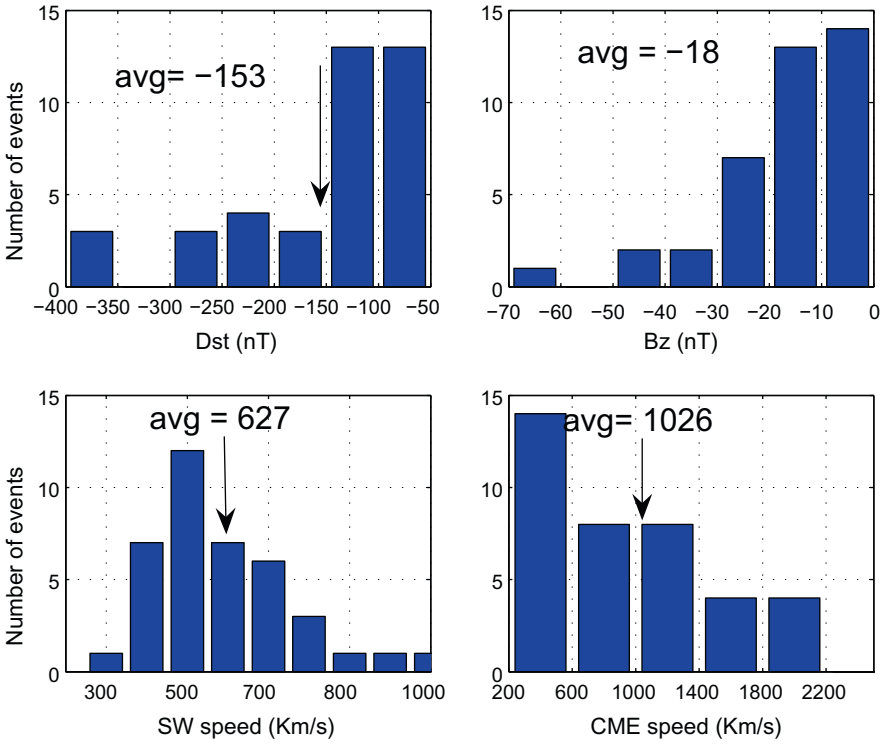


Fig. 7. Distribution of the magnitudes of *Dst*, *Bs*, SW and CMEs speeds that were associated with 39 multiple CME-driven storms.

CMEs. The CME-flare association information was available for 36 out 46 partial halo CMEs, and 38 out of 46 for full halo CMEs. Full halo CMEs were found to be generally accompanied by powerful flares of class M on the average (Fig. 5), while the majority of flares accompanying partial CMEs fall in class C on the average (Fig. 6). For partial halo CMEs, 16 of the 36 (44%) had associated solar flare surface coordinates close to the disk center, while 32 out of 38 (or 84%) of full halo CMEs originated close to the disk center. As suggested by Gopalswamy (2009), the low geoeffectiveness of partial halo CMEs compared to full halo can be attributed to the fact that they are less energetic and originate far from the disk center.

### 4.3. Multiple halo CME-associated storms

As mentioned before, cases of one storm being associated with more than one halo CME are common although in such cases of interacting geoeffective CMEs, Kim et al. (2010) noted the ambiguity to set a CME-storm relationship. In this analysis, 39 cases of multiple CME-associated storms (see Table 1) were identified representing a fraction

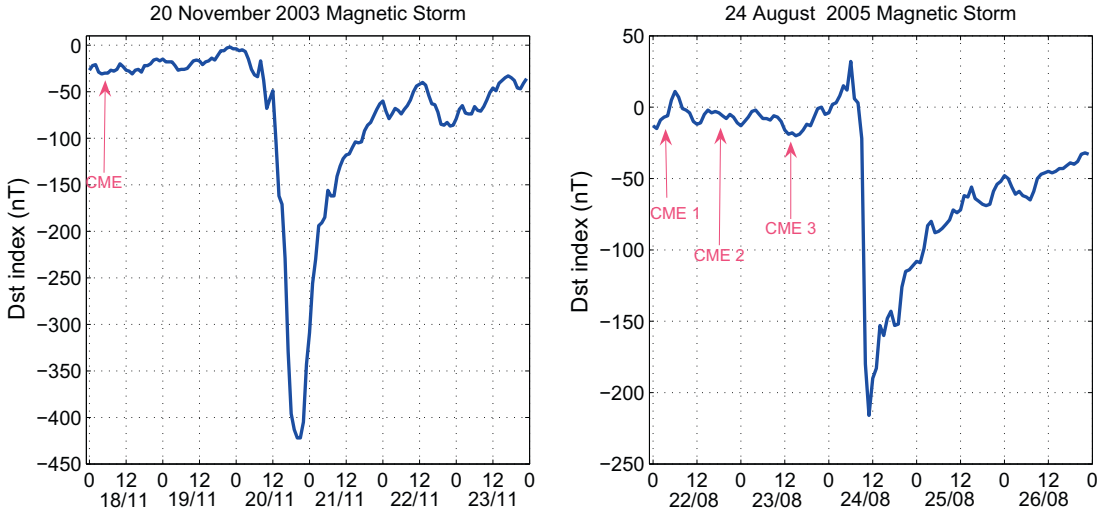


Fig. 8. Two examples showing a single and multiple CME-driven storm events.

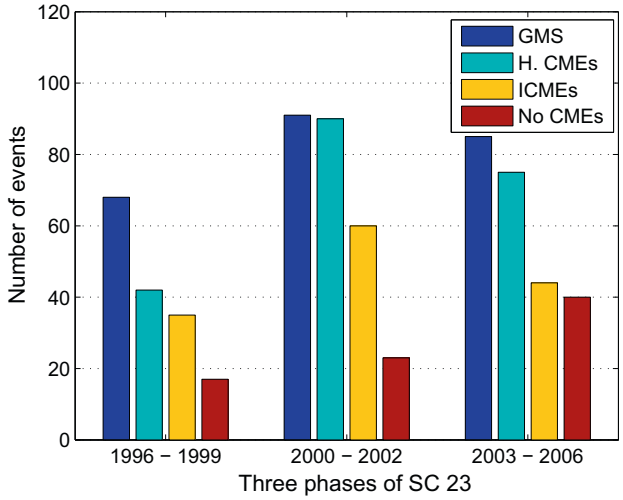


Fig. 9. Illustration of the frequency occurrence of GMS and associated halo CMEs, ICMEs and non halo CMEs associated storms in SC 23: 4 years of rising phase, 3 years of solar maximum and 4 years of declining phase.

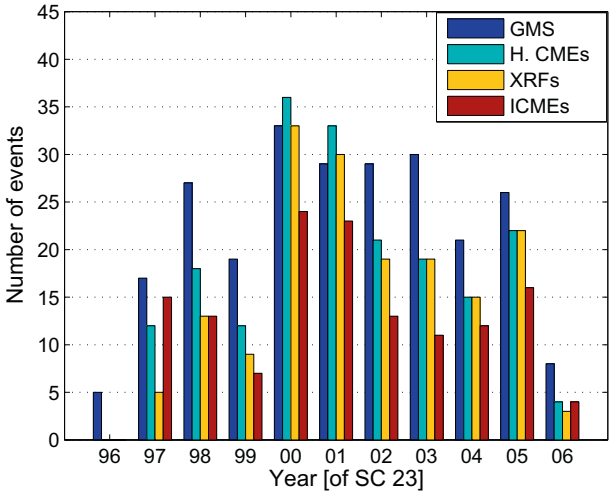


Fig. 10. A bar graph showing the frequency occurrence (per year in SC 23) of GMS with associated halo CMEs, X-ray flares and ICME events.

of 26% of all 149 CME-driven storms. The majority of these multiple CME-driven storms were intense storms [27 of 39 or 69%]. Fig. 7 shows that multiple CME-driven storms were generally associated with higher average values of *Bs*, SW and CMEs speeds. In addition, most of multiple CME-driven storms [36 out of 39 or 92%] were found to be associated with ICMEs at 1 AU. Previous studies (e.g., Xie et al., 2006; Gopalswamy, 2006) have also found a linear correlation between the intensity and duration of GMS with interacting CMEs. However, although interacting CMEs are often possible sources of the strongest storms (Yermolaev and Yermolaev, 2008), a severe storm may not always be associated with multiple halo CMEs as illustrated in Fig. 8. The greatest storm in SC 23 was a single CME-driven storm event.

### 4.4. Trends in SC 23

The SC trends of GMS and associated solar and IP sources was analysed throughout SC 23. Fig. 1 also indicates the correlation between the solar activity (expressed in terms of sunspot number) and the frequency occurrence of magnetic storms during the last three SCs. In particular, one can notice the triple peak of GMS activity as a function of SC as reported in previous studies (e.g., Yermolaev and Yermolaev, 2006). Looking at SC 23 period for which CME data records are consistently available, it is interesting to observe in Fig. 1 that the triple peak manifests also in halo CME occurrence, a trend which was also previously reported in an analysis by Gopalswamy et al. (2007).

In Fig. 9 the first 2 bars indicate the distribution of GMS and associated halo CMEs. The following two bars show the fraction of GMS that were associated with ICMEs and CIRs respectively. The distribution is shown during the rising phase (1996–1999); the maximum (2000–2002) and the declining phase (2003–2006) of SC 23. It can be seen from the figure that the majority of GMS and associated halo CMEs, ICMEs was concentrated within three years of solar maximum period: 2000, 2001 and 2002, followed by the declining phase. Fig. 9 also shows that a half (50%) of all 80 non halo CME-driven storms were concentrated within the declining phase. This is due to the fact that, in addition to the CME-driven storms, the declining phase often includes the recurrent GMS associated with the quasi-stationary corotating high speed SW streams originating in the coronal holes (Snyder et al., 1963; Kriger et al., 1973). Fig. 10 illustrates the frequency occurrence per year (in SC 23) for 244 GMS events, 192 associated halo CMEs, 183 geoeffective X-ray solar flares and 138 ICME events. The the peaks in GMS, associated CMEs and ICMEs are observed in year 1998 (rising phase), 2000-2002 (maximum phase) and 2005 (descending phase). The peak observed in year 2003 represents an exception which was also reported by Gopalswamy et al. (2007). As indicated by Hady (2009), the exceptional secondary peak observed in the declining phase of SC 23 was associated to series of solar explosive activities (Halloween storms) which occurred during the period October 17–November 10, 2003. Hady (2009) described the phenomena as being related to the large area of the active region AR 10486 and to a very strong magnetic field.

## 5. Summary

This paper described and presented results of an investigation of the probable solar sources and associated IP properties for 229 GMS events identified during SC 23. A particular aspect of these results is that they represent an estimate of probable sources of GMS within an entire 11-year average of SC activity. While previous similar studies focused on the sources of intense storms (e.g., Zhang et al., 2007), the present study has extended the analysis to moderate storms. In addition, this study provides a comparative estimate of the storm effectiveness resulting from

both full and partial halo CMEs. A 'comprehensive' list of storms together with associated solar and IP properties is provided in Table 1. The following are the main results of the analysis:

- The results obtained show that most of intense GMS (about 83%) during the period of study were caused by halo CMEs. For moderate storms, about 54% were associated with halo CMEs, while the remaining 46% have been assumed to be associated with CIRs or undetected geoeffective CMEs.
- The association with ICMEs at 1 AU is very high (86%) for intense storms, compared to moderate storms for which only 44% of them were associated with ICMEs. Note that for intense storms, the obtained percentage of ICME-storm association is comparable to the value of 87% obtained by Zhang et al. (2007).
- This investigation also indicates that nearly 69% of intense storms were caused by CMEs originating close to the disk center [within $\pm 45^{\circ}$ of the CMD], while only 51% of moderate storms had solar sources close to disk center.
- There was no significant difference between intense and moderate storms with regards to the class of X-ray flares associated to the corresponding driving halo CMEs. Generally, both intense and moderate storms were mostly associated with C and M class flares.
- A comparative analysis between partial and full halo CME-driven GMS shows that storms associated with full halo CMEs were generally intense storms with an average *Dst* of $-128$ nT, while the storms associated with partial halo CMEs were moderate with an average *Dst* of $-92$ nT. On the other hand, geoeffective parameters including the *Bs*, SW and CME speeds have been found with higher values for storms associated with full halo CMEs compared to those associated with partial halo CMEs. In addition, full halo CMEs-driven storms were associated with class M flares on average, while partial halo CME-driven storms were generally associated with C-class flares.
- Full halo CME-driven storms were associated with CMEs originating mostly close to the disk center at 84%, while only 44% of partial halo CME-driven storms were associated with CMEs originating within $\pm 45^{\circ}$ of the CMD.
- In addition, this investigation indicated that GMS possibly resulting from interacting CMEs represent 26% of all CME-driven storms, among which (69%) were intense storms. On the other hand, 92% of interacting CME-driven storms were found to be associated with ICMEs at 1 AU.
- GMS and related solar and IP properties demonstrate a triple peak during SC 23. The peaks are observed in each phase, rising phase (1998) maximum phase (2000) and declining phase (2005). Finally, this study shows that half of all no halo CME-driven storms (50%) were all concentrated in the descending phase of SC 23.

The results presented in this paper are of significant importance for the long term space weather modelling and prediction.

## Acknowledgments

We would like to thank both the National Space Science Data Center and the National Geophysical Data Center (USA) for making available their data to us via the following websites:

http://www.nssdc.gsfc.nasa/omniweb.html, ftp://ftp.ngdc.noaa.gov/STP/GEOMAG/dst.html and http://www.ngdc.noaa.gov/stp/solar/solarflares.html. The LASCO/CME catalog list used in this study is generated by NASA and the Catholic University of America in collaboration with the Naval Research Laboratory (http://cdaw.gsfc.nasa.gov/CME_list/). This work was carried out with financial support from the National Astrophysics and Space Science Programme (NASSP) and logistic support from the Space Science Directorate of the South African National Space Agency (SANSA), in Hermanus, South Africa.

## References

Brueckner, G.E., Howard, R.A., Koomen, M.J., Korendyke, C.M., Michels, D.J., Moses, J.D., Socker, D.G., Dere, K.P., Lamy, P.L., Lleberia, A., Bout, M.V., Schwenn, R., Simnett, G.M., Bedford, D.K., Eyles, C.J. The Large Angle Spectroscopic Coronagraph, (LASCO). Solar Phys. 162, 357–402, 1995.

Brueckner, G.E., Delaboudiere, J.P., Howard, R.A., Paswaters, S.E., Cyr, O.C.S., Schwenn, R., Lamy, P., Simnett, G.M., Thompson, B., Wang, D. Geomagnetic storms caused by coronal mass ejections(CMEs): March 1996 through June 1997. Geophys. Res. Lett. 25 (3019), 1998.

Cane, H.V., Richardson, I.G. Interplanetary coronal mass ejections in the near-Earth solar wind during 1996–2002. J. Geophys. Res. 108 (A4), 1156, 2003.

Crooker, N.U., McAllister, A.H. Transients associated with recurrent storms. J. Geophys. Res. 102 (14), 041, 1997.

Cyr, O.C., Howard, R.A., Sheeley, N.R., Plunkett, S.P., Michels, D.J., Paswaters, S.E., Koomen, M.J., Simnett, G.M. Properties of coronal mass ejections: SOHO LASCO observations from January 1996 to June 1998. J. Geophys. Res. 105, 169–185, 2000.

Echer, E., Gonzalez, W.D., Tsurutani, B.T., Gonzalez, A.L.C. Interplanetary conditions causing intense geomagnetic storms ($Dst \leqslant -100$ nT) during solar cycle 23 (1996–2006). J. Geophys. Res. 113 (doi:10.1029/2007JA012744), A05221, 2008.

Gonzalez, W.D., Joselyn, J.A., Kamide, Y., Kroehl, H.W., Tsurutani, B.T., Vasyliunas, V.M., Rostoker, G. What is a Geomagnetic storm? J. Geophys. Res. 99, 5771–5792, 1994.

Gopalswamy, N. Properties of interplanetary coronal mass ejections. Space Sci. Rev., 124, doi:10.1007/s 11214-006-9102-1, 2006.

Gopalswamy, N. Halo coronal mass ejections and geomagnetic storms. Earth Planets Space 61, 1–3, 2009.

Gopalswamy, N., Yashiro, S., Akiyama, S. Geoeffectiveness of halo coronal mass ejections. J. Geophys. Res. 112 (A06112), http://dx.doi.org/10.1029/2006JA012149, 2007.

Gosling, J.T., Bame, S.J., McComas, D.J., Philips, J.L. Coronal mass ejections and large geomagnetic storms. Geophys. Res. Lett. 17, 901–904, 1990.

Hady, A.A. Descriptive study of solar activity sudden increase and Hallloween storms of 2003. J. Atmos. Solar-Terres. Phys. 71, 1711–1716, 2009.

Howard, R.A., Michels, D.J., Sheeley Jr., N.R., Koomen, M.J. The observation of a coronal transient directed at Earth. Astrophys. J. 263, L101–L104, 1982.

Kahler, S.W. Solar Flares and Coronal mass Ejections. Ann. Rev. Astron. Astrophys. 30, 111–141, 1992.

Kim, R.S., Chao, K.S., Moon, Y.J., Dryer, M., Lee, J., Yi, Y., Kim, K.H., Wang, H., Park, Y.D., Kim, Y.H. An empirical model for prediction of geomagnetic storms using initially observed CME parameters at the Sun. J. Geophys. Res. A12108, http://dx.doi.org/10.1029/2010JA015322, 2010.

Kriger, A.S., Timothy, A.F., Roelf, E.C. A Coronal hole stream. Solar Phys. 29, 505, 1973.

Lanzerotti, L.J. Space weather, in: Kamide, Y., Chian, A. (Eds.), Handbook of the Solar-Terrestrial Environment. Springer-Verlag, Berlin, Heidelberg, pp. 423–443, 2007.

Loewe, C.A., Prölss, G.W. Classification and mean behaviour of magnetic storms. J. Geophys. Res. 102 (14), 209, 1997.

Messerotti, M., Zuccarello, F., Guglielmo, S.L., Bothmer, V., Lilensten, J., Noci, G., Storini, M., Lundstedt, H. Solar Weather Event Modelling and prediction. Space Sci. Rev. (DOI 10.1007/s 147, 121–185, 2009.

Richardson, I.G., Cane, H.V. Near-Earth Interplanetary Coronal Mass Ejections During Solar Cycle 23 (1996–2009): Catalog and Summary of Properties. Solar Phys. 264, 189–237, 2010.

Richardson, I.G., Cane, H.V. Geoeffectiveness (Dst and Kp) of interplanetary coronal mass ejections during 1995-2009 and the implications for storm forecasting. Space Weather 9 (S07005), http://dx.doi.org/10.1029/2011SW000670, 2011.

Richardson, I.G., Zhang, J. Multiple step geomagnetic storms and their interplanetary drivers. Geophys. Res. Lett. 35 (L06S07), http://dx.doi.org/10.1029/2007GL032025, 2008.

Richardson, I.G., Cane, H.V., Cliver, E.W. Sources of geomagnetic activity during nearly three solar cycles (1972-2000). J. Geophys. Res. 107 (A8 1187), http://dx.doi.org/10.1029/2001JA000504, 2002.

Richardson, I.G., Webb, D.F., Zhang, J., Berdichersky, D.B., Biesecker, D.A., Kasper, J.C., Kataoka, R., Steinberg, J.T., Thompson, B.J., Wu, C.-C., Zhukov, A.N. Major geomagnetic storms ($Dst \leqslant -100$ nT) generated by corotating interactive regions. J. Geophys. Res. 111 (A07S09), http://dx.doi.org/10.1029/2005 JA011476, 2006.

Robbrecht, E., Patsourakos, S., Voulidas, A. No trace left behind: STEREO observation of a coronal mass ejection without low coronal signatures. Astrophys. J. 701, 283–291, 2009.

Schwenn, R., Lago, A.D., Huttunen, E., Gonzalez, W.D. The association of coronal mass ejection with their effects near the Earth. Ann. Geophys. 23, 1033–1059, 2005.

Sheeley, N.R., Howard, R.A., Koomen, M.J., Michels, D.J., Schweenn, R., Muhlhuser, K.H., Rosenbaur, H. Coronal mass ejections and interplanetary shocks. Ann. Geophys. 90, 163, 1985.

Snyder, C.W., Neugebauer, M., Rao, U.R. The solar wind velocity and its correlation with cosmic-ray variation and with solar and geomagnetic activity. J. Geophys. Res. 68, 6361–6370, 1963.

Tsurutani, B.T., Gonzalez, W.D., 1997. The interplanetary causes of magnetic storms: a review. In: Tsurutani, B.T., Gonzalez, W.D., Kamide, Y., Arballo, J.K. (Eds.), Magnetic Storms, vol. 98 of Geophysical Monograph Series. AGU, Washington DC, pp. 77–89.

Uwamahoro, J., McKinnell, L.A., Habarulema, J.B. Estimating the geoeffectiveness of halo CMEs from associated solar and IP parameters using neural networks. Ann. Geophys. 30, 963–972, 2012.

Wang, Y.M., Ye, P.Z., Wang, S., Zhou, G.P., Wang, J.X. A statistical study on the geoeffectiveness of the Earth-directed coronal mass ejections from March 1997 to December 2000. J. Geophys. Res. 107 (A11), 1340, 2002.

Wang, Y., Chen, C., Gui, B., Shen, C., Ye, P., Wang, S. Statistical study of coronal mass ejection source locations: Understanding CMEs viewed in coronagraphs. J. Geophys. Res. 116 (A04104), http://dx.doi.org/10.1029/2010JA016101,2011, 2011.

Webb, D.F., Cliver, E.W., Crooker, N.U., st Cyr, O.C., Thompson, B.J. Relationship of halo coronal mass ejections, magnetic clouds and magnetic storms. J. Geophys. Res. 105, 7491, 2000.

Xie, H., Gopalswamy, N., Manoharan, P.K., Lara, A., Yashiro, S., Lepri, S. Long-lived geomagnetic storms and coronal mass ejections. J. Geophys. Res., 111. A01103, 2006.

Yashiro, S., Gopalswamy, N., Michalek, G., Cyr, O.C.S., Plunkett, S.P., Rich, N.B., Howard, R.A. A catalog of white light coronal mass ejections observed by the SOHO spacecraft. J. Geophys. Res. 109 (A07105), http://dx.doi.org/10.1029/2003JA010282, 2004.

Yermolaev, Y.I., Yermolaev, M.Y. Statistical study on geomagnetic storm effectiveness of solar and interplanetary events. Advance, s in Space Research 37, 6), 1175–1181, 2006.

Yermolaev, Y.I., Yermolaev, M.Y. Solar and interplanetary sources of geomagnetic storms: space weather aspects. Izvestiya Atmos. Ocean. Phys. 46 (7), 799–819, 2010.

Yermolaev, I.Y., Yermolaev, M.Y., Zastenker, G.N., Zelenyi, L.M., Petrucovich, A., Sauvaud, J.A. Statistical studies of geomagnetic storm dependencies on solar and and interplanetary events: a review. Planet. Space Sci. 53, 189–196, 2005.

Yermolaev, Y.I., Yermolaev, M.Y., Gonzalez, D., et al. Comments on "Interplanetary origin of intense geomagnetic storms ($Dst < -100$ nT) during Solar Cycle 23 by W. Geophys. Res. Lett. 35 (L01101), http://dx.doi.org/10.1029/2007 GL030281, 2008.

Zhang, J., Richardson, I.G., Webb, D.F., Gopalswamy, N., Huttunen, E., Kasper, J.C., Nitta, N.V., Poomvises, W., Thompson, B.J., Wu, C.C., Yashiro, S., Zhukov, A.N. Solar and interplanetary sources of major geomagnetic storms ($Dst \leqslant -50$ nT) during 1996–2005. J. Geophys. Res. 112 (A10102), http://dx.doi.org/10.1029/2007JA012321, 2007.